Cell, Vol. 82, 415–424, August 11, 1995,

Decoding of Cytosolic Calcium Oscillations in the Mitochondria

György Hajnóczky, Lawrence D. Robb-Gaspers, Michele B. Seitz, and Andrew P. Thomas
Department of Pathology
Anatomy and Cell Biology
Thomas Jefferson University
Philadelphia, Pennsylvania 19107

Summary

Frequency-modulated oscillations of cytosolic Ca^{2+} ($[Ca^{2+}]_c$) are believed to be important in signal transduction, but it has been difficult to correlate $[Ca^{2+}]_c$ oscillations directly with the activity of Ca^{2+}-regulated targets. We have studied the control of Ca^{2+}-sensitive mitochondrial dehydrogenases (CSMDHs) by monitoring mitochondrial Ca^{2+} ($[Ca^{2+}]_m$) and the redox state of flavoproteins and pyridine nucleotides simultaneously with $[Ca^{2+}]_c$ in single hepatocytes. Oscillations of $[Ca^{2+}]_c$ induced by IP_3-dependent hormones were efficiently transmitted to the mitochondria as $[Ca^{2+}]_m$ oscillations. Each $[Ca^{2+}]_m$ spike was sufficient to cause a maximal transient activation of the CSMDHs and $[Ca^{2+}]_m$ oscillations at frequencies above 0.5 per minute caused a sustained activation of mitochondrial metabolism. By contrast, sustained $[Ca^{2+}]_c$ increases yielded only transient CSMDH activation, and slow or partial $[Ca^{2+}]_c$ elevations were ineffective in increasing $[Ca^{2+}]_m$ or stimulating CSMDHs. We conclude that the mitochondria are tuned to oscillating $[Ca^{2+}]_c$ signals, the frequency of which can control the CSMDHs over the full range of potential activities.

Introduction

The cytosolic Ca^{2+} ($[Ca^{2+}]_c$) signals that mediate the effects of many extracellular stimuli occur in the form of frequency-modulated and spatially organized $[Ca^{2+}]_c$ oscillations in the individual cells (Rapp and Berridge, 1981; Woods et al., 1986; Rooney et al., 1989, 1990). Frequency modulation of rapid and relatively large $[Ca^{2+}]_c$ oscillations may serve to discriminate the agonist-induced $[Ca^{2+}]_c$ signals from background $[Ca^{2+}]_c$ changes at the level of Ca^{2+}-sensitive proteins. However, it is unclear exactly how the repetitive $[Ca^{2+}]_c$ spikes are recognized by target proteins in the cytoplasm or in intracellular compartments (Meyer and Stryer, 1991). Oscillations of $[Ca^{2+}]_c$ may be expected to yield a variety of response patterns in the Ca^{2+}-sensitive targets, ranging from activities that are closely entrained to the periodic $[Ca^{2+}]_c$ changes to situations in which a steady state or slow ramp of activity occurs. A complex relationship between $[Ca^{2+}]_c$ and a Ca^{2+}-regulated process may also occur when activation and inactivation are controlled by independent Ca^{2+}-sensitive pathways. Importantly, although $[Ca^{2+}]_c$ spikes may be of insufficient duration to evoke a full response, a sustained $[Ca^{2+}]_c$ increase is expected to be at least as potent as $[Ca^{2+}]_c$ oscillations.

Another feature of intracellular Ca^{2+} signaling that may play a role in targeting the regulatory effects of Ca^{2+} is the spatial organization of $[Ca^{2+}]_c$ changes (Thomas et al., 1992). It has been suggested that "strategic localization" of Ca^{2+} release sites at the subcellular level may give rise to selective activation of specific processes (Robitaille et al., 1990; Rizzuto et al., 1993). Thus, localized high levels of $[Ca^{2+}]_c$ generated in the immediate vicinity of intracellular or plasmalemmal Ca^{2+} channels may yield rapid and spatially limited changes in the activity of Ca^{2+}-regulated processes, despite the eventual spread of the $[Ca^{2+}]_c$ increase to more distal parts of the cell.

It is clear that characterization of the effects of $[Ca^{2+}]_c$ oscillations in situ is required to understand the physiological process by which these complex signals are decoded. In addition to the difficulties inherent in monitoring the function of Ca^{2+}-sensitive proteins at the level of single cells, a number of Ca^{2+}-sensitive targets are compartmentalized within intracellular organelles such as the nucleus (Bachs et al., 1992) and the mitochondria (Denton and McCormack, 1980; Hansford, 1980). In the case of mitochondria, specific Ca^{2+} transport pathways regulate mitochondrial matrix free Ca^{2+} concentration ($[Ca^{2+}]_m$). The uptake of Ca^{2+} is driven by the membrane potential mediated by an electrogenic uniport, and efflux of mitochondrial Ca^{2+} occurs via Na^+-independent and Na^+-dependent carriers. There have been relatively few studies of the relationship between $[Ca^{2+}]_c$ and $[Ca^{2+}]_m$ in intact cells. In electrically paced cardiac myocytes, $[Ca^{2+}]_c$ transients occurring in the subsecond time domain were not reflected individually in measurable $[Ca^{2+}]_m$ spikes, but the steady-state level of $[Ca^{2+}]_m$ was a function of the pacing frequency (Miyata et al., 1991). Rizzuto et al. (1992, 1993, 1994) have measured $[Ca^{2+}]_m$ by expression of chimeric Ca^{2+}-sensitive photoproteins targeted to mitochondria. This approach has demonstrated increases of $[Ca^{2+}]_m$ occurring simultaneously with $[Ca^{2+}]_c$ increases in cell populations. However, it has not yet been possible to detect $[Ca^{2+}]_m$ signals at the level of individual cells, which is an essential requirement for characterizing how the asynchronous oscillations of $[Ca^{2+}]_c$ are transduced into changes in $[Ca^{2+}]_m$.

The aim of the present study was to determine how inositol 1,4,5-trisphosphate (IP_3)-dependent $[Ca^{2+}]_c$ oscillations are transmitted to the mitochondria and to investigate the relationship between the oscillating Ca^{2+} signals and the activity of mitochondrial Ca^{2+}–sensitive enzymes. We have taken advantage of the fact that Ca^{2+} regulates several mitochondrial dehydrogenases, the activity of which can be monitored fluorometrically through changes in the redox state of their flavin and pyridine nucleotide cofactors. This approach has allowed us to obtain real time spatially resolved imaging measurements of the activity of the Ca^{2+}-sensitive mitochondrial dehydrogenases (CSMDHs) from single living cells. Three CSMDHs are known to be regulated by $[Ca^{2+}]_m$ in the nanomolar to micromolar range expected in the matrix of mitochondria in healthy intact cells (Denton and McCormack, 1980; Hansford, 1980;

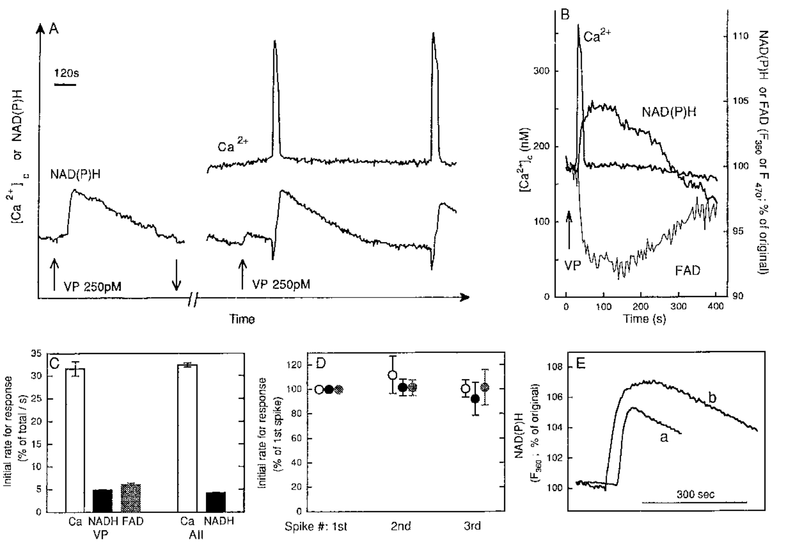

Figure 1. Relationship among NAD(P)H, $FADH_2$, and $[Ca^{2+}]_c$ Oscillations in Individual Hepatocytes

(A) The NAD(P)H increase induced by a low dose of vasopressin (VP) was measured before Fura 2 loading (left trace). The cell was then loaded with a low level of Fura 2, and NAD(P)H and $[Ca^{2+}]_c$ were monitored simultaneously during restimulation with vasopressin.

(B) NAD(P)H, FAD, and $[Ca^{2+}]_c$ measured simultaneously during a $[Ca^{2+}]_c$ spike induced by 100 pM vasopressin (VP).

(C) Initial rates of NAD(P)H, $FADH_2$, and $[Ca^{2+}]_c$ increase induced by 100–200 pM vasopressin (VP) and 200–500 pM angiotensin II (AII) were normalized to the magnitude of the total response. Calculated rates are mean ± SEM of values from 80–100 cells from four to five different cultures.

(D) Comparison of the initial rates of the first, second, and third NAD(P)H, $FADH_2$, and $[Ca^{2+}]_c$ spikes during vasopressin-induced oscillations.

(E) Comparison of NAD(P)H increases during oscillatory and sustained $[Ca^{2+}]_c$ responses. Cells were stimulated first with 80 pM vasopressin, resulting in low frequency $[Ca^{2+}]_c$ oscillations (trace a), and then with 20 nM vasopressin to yield a sustained $[Ca^{2+}]_c$ response (trace b). The traces represent mean values calculated by synchronizing the rising phase of $[Ca^{2+}]_c$; both traces were averaged from the same cells.

McCormack et al., 1990). Nicotinamide adenine dinucleotide (NAD) isocitrate dehydrogenase and oxoglutarate dehydrogenase (OGDH) are allosterically regulated by Ca^{2+}, whereas pyruvate dehydrogenase (PDH) is under phosphorylation control by a kinase (which inactivates PDH) and a Ca^{2+}-stimulated phosphatase (which activates PDH). All three CSMDHs catalyze the reduction of NAD to reduced nicotinamide adenine dinucleotide (NADH), and the OGDH and PDH enzyme complexes contain a flavoprotein, lipoamide dehydrogenase, that transfers the reducing equivalents via reduced flavin adenine dinucleotide ($FADH_2$) to NADH. NADH is a key intermediate supplying reducing equivalents to the mitochondrial respiratory chain for ATP synthesis, and the ratio of NADH to NAD regulates numerous metabolic and synthetic enzymes through both active site and allosteric interactions.

Previous studies have demonstrated that NAD(P)H fluorescence signals and Ca^{2+}-induced changes in the pyridine nucleotide redox state can be measured at the level of individual cells (Pralong et al., 1992, 1994). Although direct control of these redox reactions by Ca^{2+} is only known to occur in the mitochondria (through the CSMDHs), NAD(P)H fluorescence is derived from several intracellular compartments, and this parameter may also be influenced by indirect regulatory effects of $[Ca^{2+}]_c$. By contrast, FAD fluorescence is predominantly mitochondrial, and the presence of an intrinsic FAD-containing flavoprotein component in OGDH and PDH allows the redox state of the flavins to act as a direct indicator of dehydrogenase activity (Scholz et al., 1969). Therefore, the activity of the CSMDHs was followed by monitoring the redox state of both the pyridine and flavin nucleotides and was correlated with $[Ca^{2+}]_c$ and $[Ca^{2+}]_m$ changes induced by oscillatory and nonoscillatory hormone doses and by the Ca^{2+} pump inhibitor thapsigargin. $[Ca^{2+}]_c$ levels were measured using Fura 2, and changes in $[Ca^{2+}]_m$ were measured using the fluorescent Ca^{2+} indicator Rhod 2 preferentially compartmentalized in the mitochondrial matrix (Mix et al., 1994). The combination of these approaches has allowed us to demonstrate that the pulsatile release of Ca^{2+} underlying $[Ca^{2+}]_c$ oscillations is transmitted efficiently into the mitochondrial matrix, giving rise to associated oscillations of $[Ca^{2+}]_m$. Sustained stimulation of CSMDHs can be achieved in the upper range of $[Ca^{2+}]_c$ and $[Ca^{2+}]_m$ oscillation frequencies. By contrast, a nonoscillatory-sustained $[Ca^{2+}]_c$ increase resulting from maximal hormonal stimulation of the cells evokes only transient $[Ca^{2+}]_m$ and redox responses, despite the persistence of the $[Ca^{2+}]_c$ signal.

Results and Discussion

Oscillations of $[Ca^{2+}]_c$ and Redox State

Hormone-induced changes in the redox state of pyridine and flavin nucleotides were monitored in individual hepatocytes. Reduction of the NAD(P)/NAD(P)H couple is associated with increased fluorescence (360 nm excitation), whereas reduction of the FAD/$FADH_2$ pair results in a decrease in fluorescence (470 nm excitation). Figure 1A shows a transient increase in pyridine nucleotide fluorescence in response to stimulation by vasopressin in a hepatocyte prior to loading with fluorescent Ca^{2+} indicator. The temporal relationship between the increases of NAD(P)H and the $[Ca^{2+}]_c$ oscillations was then determined by loading the same cells with Fura 2 and monitoring the fluorescence signals due to NAD(P)H and $[Ca^{2+}]_c$ simultaneously. Figure 1A (right traces) shows that the NAD(P)H transients were synchronized to the individual spikes of the $[Ca^{2+}]_c$ oscillations during restimulation with vasopressin. Closer examination of the kinetics during a single $[Ca^{2+}]_c$ spike reveals that the rising phase of the NAD(P)H increase lags slightly behind the $[Ca^{2+}]_c$ increase (Figure 1B). The declining phase of NAD(P)H fluorescence was considerably slower than for the $[Ca^{2+}]_c$ spike. Each NAD(P)H oscillation was paralleled by a transient reduction of FAD (manifest as a

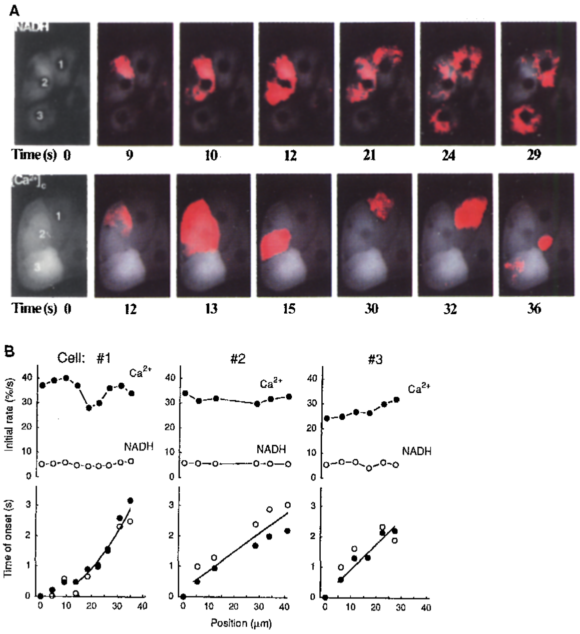

Figure 2. Spatial Organization of NAD(P)H and $[Ca^{2+}]_c$ Changes Induced by Vasopressin in Individual Hepatocytes

(A) The gray images show the NAD(P)H fluorescence (top row) and Fura 2 fluorescence (bottom row) in three individual hepatocytes challenged with vasopressin (5 nM). The red overlays show the fluorescence change at each timepoint, calculated by subtraction of sequential images (Robb-Gaspers and Thomas, 1995). Thus, the overlays represent a differential analysis indicating the spatial locations where NAD(P)H and $[Ca^{2+}]_c$ was increasing at each timepoint. Times are shown relative to the addition of vasopressin. The NAD(P)H and $[Ca^{2+}]_c$ waves induced by vasopressin were measured in sequential runs: first, NAD(P)H was measured in unloaded cells with 360 nm excitation, and then after washout of the vasopressin and loading with Fura 2, the $[Ca^{2+}]_c$ waves were measured with 380 nm excitation.

(B) Initial rate and time of onset of the NAD(P)H and $[Ca^{2+}]_c$ increases are shown in different subregions of the three responsive cells from (A). The subregions for each cell were selected along the path of Ca^{2+} wave propagation. Onset times are given relative to the initiation of the $[Ca^{2+}]_c$ wave in each cell.

decrease in flavin fluorescence). Simultaneous measurement of $[Ca^{2+}]_c$, NAD(P)H, and flavoprotein fluorescence demonstrated that FAD reduction followed the rising phase of the $[Ca^{2+}]_c$ spikes, but, as with NAD(P)H, the reoxidation occurred more slowly than the recovery of $[Ca^{2+}]_c$ (Figure 1B).

Figure 1C compares the rates of rise of $[Ca^{2+}]_c$, NAD(P)H, and $FADH_2$ normalized to the peak amplitude of each response. The initial rates for the rising phase of the NAD(P)H and $FADH_2$ spikes induced by vasopressin were very similar, but about 5-fold slower than the initial rate of the $[Ca^{2+}]_c$ spikes (Figure 1C). Initial rates for consecutive $[Ca^{2+}]_c$, NAD(P)H, and $FADH_2$ spikes were found to be constant during the vasopressin-induced oscillations (Figure 1D), indicating that the declining phase of the redox oscillations is unlikely to reflect an adaptive response that counters the Ca^{2+} stimulation of the CSMDHs. Importantly, the initial rate of NAD(P)H increase was the same for both oscillatory and sustained $[Ca^{2+}]_c$ increases (Figure 1E), consistent with our earlier observations (Rooney et al., 1989) that the rate of $[Ca^{2+}]_c$ rise is independent of agonist dose throughout the oscillatory and sustained range. Furthermore, the kinetics of the redox oscillations evoked by two different Ca^{2+}-mobilizing hormones, vasopressin and angiotensin II, were the same (Figure 1C).

Spatial Relationship between $[Ca^{2+}]_c$ and NAD(P)H Oscillations in Single Hepatocytes

We have shown previously that hormone-induced $[Ca^{2+}]_c$ oscillations in hepatocytes arise in a discrete subcellular region and then propagate through the cell as a Ca^{2+} wave (Rooney et al., 1990). For each cell, the origin and path of Ca^{2+} waves are the same for all of the oscillations in a series and are conserved through multiple hormone challenges. The redox oscillations induced by Ca^{2+}-mobilizing hormones also occurred as spatially organized waves within each individual hepatocyte, and these intracellular waves of NAD(P)H reduction followed the same path as the Ca^{2+} waves measured in the same cell (Figure 2). To avoid contamination of the NAD(P)H signal by Fura 2, unloaded cells were first stimulated with vasopressin, and the NAD(P)H fluorescence changes were recorded at 360 nm (top row of images in Figure 2A). The cells were then loaded with Fura 2, and $[Ca^{2+}]_c$ was monitored using 380 nm excitation, since the Ca^{2+}-dependent decrease in Fura 2 fluorescence at this wavelength is opposite to that for NAD(P)H. In each of the three cells that gave NAD(P)H responses, restimulation with vasopressin after Fura 2 loading gave Ca^{2+} waves (bottom row of images in Figure 2A) that followed a similar spatiotemporal pattern to the NAD(P)H reduction observed during the initial stimulation. However, although the Ca^{2+} waves propagated through the nucleus (see also Lin et al., 1994), the NAD(P)H waves were excluded from the region occupied by the nucleoplasm (Figure 2).

The kinetics of Ca^{2+} and NAD(P)H wave propagation were compared by measuring the time course of fluorescence changes at a series of points along a line parallel to the direction of the waves in each cell. The top graphs in Figure 2B show the initial rates of $[Ca^{2+}]_c$ and NAD(P)H increase (normalized to peak amplitude) measured at each subcellular region for the three cells indicated in Figure 2A. The relative time of onset of the fluorescence changes at these subcellular regions during the propagation of the Ca^{2+} and NAD(P)H waves are shown in the bottom graphs in Figure 2B. As reported previously (Rooney et al., 1990; Lin et al., 1994), the $[Ca^{2+}]_c$ increases were offset in time along the path of Ca^{2+} wave propagation, but the initial rates of $[Ca^{2+}]_c$ increase were relatively constant throughout the cytoplasm. Although the initial rates of NAD(P)H increase were slower than for $[Ca^{2+}]_c$, these rates were also relatively constant along the entire path of NAD(P)H wave propagation. Moreover, the time offset for the initiation of the NAD(P)H fluorescence increase at each subcellular region was the same as for the $[Ca^{2+}]_c$ increases (bottom graphs of Figure 2B). Thus, the wave of NAD(P)H reduction closely follows the kinetics of Ca^{2+} wave propagation in hepatocytes. The calculated wave propagation rates for both parameters were 12–25 μm/s. These data suggest that the hormone-induced re-

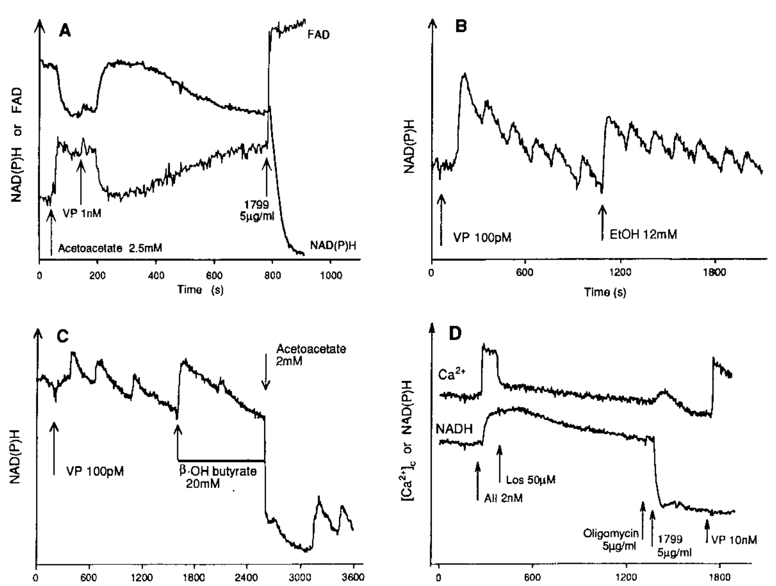

Figure 3. Mitochondrial Localization of Ca^{2+}-Induced Redox Responses

(A) NAD(P)H and FAD fluorescence were monitored simultaneously in a single hepatocyte. Acetoacetate was added to oxidize mitochondrial pyridine and flavin nucleotides prior to stimulation with vasopressin (VP). The dose of 1 nM vasopressin caused a sustained increase of $[Ca^{2+}]_c$ in this experiment. The uncoupler 1799 was used to stimulate mitochondrial oxidation.

(B) Effect of cytosolic NAD reduction by ethanol (EtOH) on vasopressin (VP)-induced NAD(P)H oscillations. The initial decline in fluorescence after vasopressin addition reflects photobleaching in this cell.

(C) Effect of reduction and oxidation of mitochondrial NAD by β-hydroxybutyrate (β-OH butyrate) and acetoacetate on vasopressin (VP)-induced NAD(P)H oscillations.

(D) Effects of mitochondrial uncoupler on the $[Ca^{2+}]_c$ signal and NAD(P)H increase induced by IP_3-linked stimuli. NAD(P)H and $[Ca^{2+}]_c$ were monitored simultaneously in a single hepatocyte. Angiotensin II (AII) induced an increase of $[Ca^{2+}]_c$, which was reversed by the antagonist losartan K (Los). Oligomycin was added prior to the uncoupler to inhibit mitochondrial hydrolysis of cellular ATP. VP, vasopressin.

dox responses of the cell are controlled locally at the subcellular sites of Ca^{2+} mobilization.

Mitochondrial Localization of Redox Changes

The flavin fluorescence signal is derived predominantly from the mitochondria in hepatocytes (Scholz et al., 1969), whereas both cytosolic and mitochondrial components contribute to the measured NAD(P)H fluorescence. The parallel time courses of pyridine and flavin nucleotide reduction and reoxidation during each $[Ca^{2+}]_c$ oscillation, together with the nonnuclear subcellular distribution of these redox responses, is consistent with the mitochondrial localization of the CSMDHs. As a further approach to elucidate the compartment responsible for the hormone-induced redox oscillations, hepatocytes were incubated under conditions designed selectively to perturb the mitochondrial and cytosolic redox states. Acetoacetate and β-hydroxybutyrate are interconverted by the mitochondrial matrix enzyme β-hydroxybutyrate dehydrogenase, which utilizes mitochondrial NADH and NAD. As shown in Figure 3A, addition of acetoacetate caused rapid oxidation of mitochondrial NAD(P)H (decreased fluorescence), and this was accompanied by a parallel oxidation of FAD (increased fluorescence). The changes in NAD(P)H and FAD fluorescence induced by subsequent addition of vasopressin also occurred in parallel, and these hormone-induced redox changes were proportional to the acetoacetate-induced changes. Subsequent addition of the mitochondrial uncoupler 1799 caused reoxidation of both the pyridine and flavin nucleotides (Figure 3A). The NADH reductase inhibitor rotenone also caused parallel reductions of NAD and FAD, the amplitude of which were about 3-fold greater than the hormone-induced reduction of these nucleotides (data not shown).

Figure 3C shows that vasopressin-induced NAD(P)H oscillations were blocked when β-hydroxybutyrate was added to increase mitochondrial NAD(P)H levels, and the oscillations recovered following subsequent acetoacetate addition. By contrast, reduction of the cytosolic NAD(P) pool, using ethanol to activate cytosolic alcohol dehydrogenase, had no effect on the amplitude or frequency of vasopressin-induced NAD(P)H oscillations (Figure 3B). Vasopressin-induced $[Ca^{2+}]_c$ oscillations were unaffected by acetoacetate, β-hydroxybutyrate, or ethanol (data not shown). Hormone-induced $[Ca^{2+}]_c$ responses could also be observed in the presence of uncoupler, provided that the mitochondrial ATPase inhibitor oligomycin was first added to preserve cytosolic ATP. Figure 3D shows $[Ca^{2+}]_c$ and NAD(P)H responses to angiotensin II, followed by addition of the angiotensin II antagonist losartan K and then restimulation with vasopressin after addition of oligomycin and 1799. The uncoupler caused a small transient increase in $[Ca^{2+}]_c$ and a large oxidation of mitochondrial NAD(P)H. The hormone-induced $[Ca^{2+}]_c$ change was similar before and after uncoupler treatment, but the NAD(P)H response was completely eliminated in the presence of uncoupler. Taken together, these data indicate that the redox oscillations induced by Ca^{2+}-mobilizing hormones occur in the mitochondria.

As noted above (see Figure 1), the vasopressin-induced oscillations of NAD(P)H and $FADH_2$ followed the rising phase of the $[Ca^{2+}]_c$ oscillations with only a slight lag, but these components decayed to their more oxidized basal states much more slowly than the decline of $[Ca^{2+}]_c$. This slow rate of reoxidation was observed even when a sustained $[Ca^{2+}]_c$ increase to angiotensin II was reversed with the antagonist losartan K (Figure 3D). These data indicate that increases of $[Ca^{2+}]_c$ are rapidly conveyed to the sites

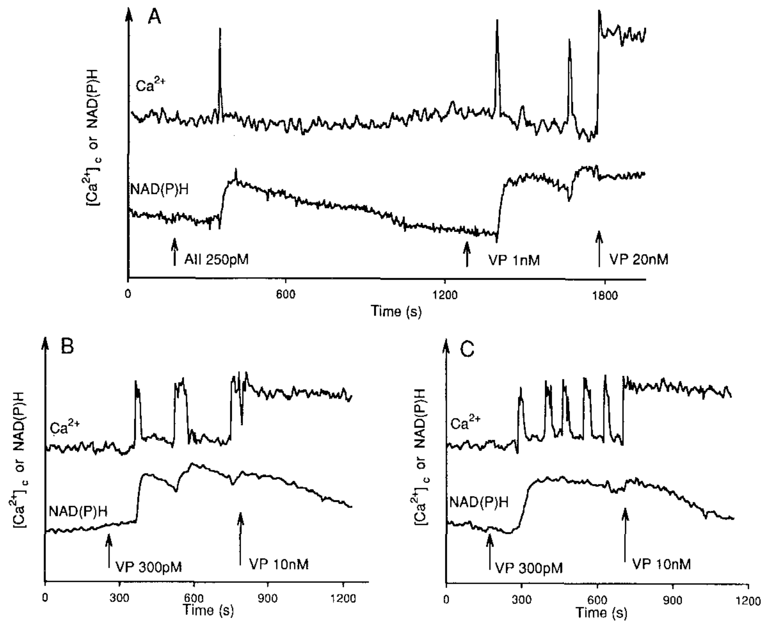

Figure 4. Relationship between the Frequency of $[Ca^{2+}]_c$ Oscillations and Mitochondrial Redox Responses

NAD(P)H and $[Ca^{2+}]_c$ changes measured simultaneously are shown for three individual hepatocytes in (A), (B), and (C), respectively, which were stimulated with angiotensin II (AII) and vasopressin (VP) at the indicated concentrations to generate $[Ca^{2+}]_c$ oscillations and sustained $[Ca^{2+}]_c$ increases.

at which Ca^{2+} stimulates the production of NAD(P)H and $FADH_2$, but a step other than the reversal of the $[Ca^{2+}]_c$ increase must be rate limiting for the return of this activity to the initial basal state. The mitochondrial compartmentation of the CSMDHs offers several potential mechanisms for this constraint on the regulation of redox state by $[Ca^{2+}]_c$. Because the mitochondria utilize separate pathways for Ca^{2+} uptake and efflux, it is possible that $[Ca^{2+}]_m$ may decrease relatively slowly compared with the falling phase of the $[Ca^{2+}]_c$ oscillations. However, our direct measurements of $[Ca^{2+}]_m$ suggest that this is not the case (see below). Alternatively, the activated state of the CSMDHs may decline more slowly than $[Ca^{2+}]_m$. The latter possibility would be most readily explained for PDH, which is activated by a Ca^{2+}-stimulated phosphatase and inactivated by a Ca^{2+}-independent kinase. It is also possible that Ca^{2+} may affect CSMDHs by additional indirect mechanisms. For example, alkalinization decreases the substrate affinity of isocitrate dehydrogenase and OGDH (Nichols et al., 1994), and Ca^{2+} mobilization is associated with marked changes of cytosolic pH in many cells. However, Ca^{2+}-mobilizing hormones do not affect cytosolic pH in hepatocytes (Anwer, 1994), although their effect on mitochondrial pH has not been elucidated.

Frequency Modulation of Mitochondrial Responses

An important feature of the mitochondrial redox oscillations is that the individual redox transients induced by repetitive $[Ca^{2+}]_c$ spiking had the same initial rate and overall shape (see Figure 1). These findings demonstrate that $[Ca^{2+}]_c$ oscillations can stimulate the CSMDHs for extended periods without desensitization or adaptation. In parallel with the modulation of $[Ca^{2+}]_c$ oscillation frequency by agonist dose, the frequency of the cycles of CSMDH activation increased with increasing stimulation intensity. However, in the higher range of $[Ca^{2+}]_c$ oscillation frequencies, the redox spikes ran together, owing to the relatively slow reoxidation phase (Figure 4). Importantly, the peak level of NAD(P)H spikes was no higher when these were superimposed on the falling phase of the preceding redox transient. Moreover, when a higher agonist dose was added during ongoing $[Ca^{2+}]_c$ and redox oscillations, the resulting out-of-phase increase in $[Ca^{2+}]_c$ was accompanied by an NAD(P)H spike sufficient to reach, but not exceed, the preceding peak NAD(P)H level (Figure 4). These data indicate that each burst of Ca^{2+} release into the cytosol was sufficient to yield a near-maximal activation of the CSMDHs. The availability of NAD(P) is unlikely to be a limiting factor in these redox measurements, because substantially larger changes in NAD(P)H and FAD fluorescence were elicited by addition of rotenone (data not shown).

Discrete mitochondrial redox spikes were observed at $[Ca^{2+}]_c$ oscillation frequencies in the range of 0.2 per minute and below. The redox spikes began to become superimposed at higher oscillation frequencies and fused into an essentially sustained NAD(P)H elevation when the $[Ca^{2+}]_c$ oscillation frequency was 0.5–1 per minute (Figure 4). Under these conditions of relatively rapid $[Ca^{2+}]_c$ spiking, NAD(P)H fluorescence remained at the peak level observed for single redox spikes, and there was no indication of decline or adaptation (Figure 4C). The redox response was remarkably different when a high agonist dose was added sufficient to cause a sustained elevation of $[Ca^{2+}]_c$. Under these conditions, NAD(P)H fluorescence increased immediately to a similar level to that observed for the oscillatory range. However, in contrast with the maintenance of the peak NAD(P)H level induced by high frequency $[Ca^{2+}]_c$ oscillations, the sustained increase in $[Ca^{2+}]_c$ caused only a transient elevation of NAD(P)H (Figures 4B and 4C). Measurements of FAD fluorescence revealed an identical pattern of response; oscillating $[Ca^{2+}]_c$ signals were associated with FAD oscillations that fused into a persistent maximal reduction at higher frequencies, whereas sustained $[Ca^{2+}]_c$ increases gave only a transient reduction of FAD (data not shown). Thus, the control of

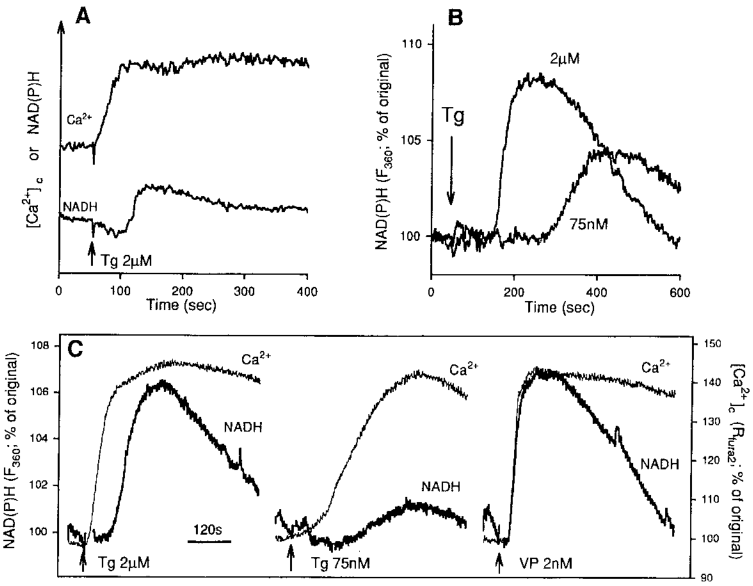

Figure 5. Effect of the Intracellular Ca^{2+} Pump Inhibitor Thapsigargin on $[Ca^{2+}]_c$ and NAD(P)H

(A) Simultaneous measurements of $[Ca^{2+}]_c$ and NAD(P)H are shown in an individual hepatocyte exposed to thapsigargin (Tg).

(B) NAD(P)H increases in response to maximum (2 μM) and low dose (75 nM) thapsigargin (Tg) in individual hepatocytes.

(C) Mean increases in $[Ca^{2+}]_c$ and NAD(P)H in hepatocytes challenged with maximal and low doses of thapsigargin (Tg) or 2 nM vasopressin (VP) are shown. The mean traces for NAD(P)H and $[Ca^{2+}]_c$ are from separate runs using cells from the same primary culture. All cells in the field were included for calculation of the mean responses.

the CSMDHs appears to reflect a unique situation in which $[Ca^{2+}]_c$ oscillations are an effective signal for long-term activation, but nonoscillatory $[Ca^{2+}]_c$ increases in response to higher hormone doses fail to sustain the activated state, even though $[Ca^{2+}]_c$ remains at the same level achieved during the peak of the $[Ca^{2+}]_c$ oscillations.

Transmission of $[Ca^{2+}]_c$ Signals to the Mitochondrial Matrix

One potential explanation for the observation that $[Ca^{2+}]_c$ oscillations are more effective in CSMDH activation than a sustained $[Ca^{2+}]_c$ increase of similar amplitude is that the process of Ca^{2+} release from intracellular stores may itself be important in transmitting the $[Ca^{2+}]_c$ signal into the mitochondria. Rizzuto et al. (1993) used aequorin targeted to the mitochondria in cell population measurements to demonstrate that Ca^{2+} released to the cytosol in response to IP_3 is transferred into the mitochondrial matrix much more effectively than $[Ca^{2+}]_c$ increases induced by other means. These data were taken to indicate a close relationship between the sites of IP_3-induced Ca^{2+} mobilization and the mitochondrial Ca^{2+} uptake sites. To investigate whether the activation of CSMDHs in hepatocytes was similarly coupled to IP_3-mediated Ca^{2+} release, we examined the effect of thapsigargin. This agent inhibits the intracellular Ca^{2+} pump and causes $[Ca^{2+}]_c$ to rise as a result of Ca^{2+} leakage from intracellular stores.

Figure 5A shows simultaneous measurements of $[Ca^{2+}]_c$ and NAD(P)H changes induced by a maximal dose of thapsigargin, and mean traces for these parameters are shown on the left in Figure 5C. After thapsigargin addition, $[Ca^{2+}]_c$ increased without any significant delay to a level that was similar to that observed at the peak of the vasopressin response (right set of traces in Figure 5C). The rate of $[Ca^{2+}]_c$ increase was slower with thapsigargin than with vasopressin. At submaximal thapsigargin doses, $[Ca^{2+}]_c$ increased even more slowly, but still attained the same peak level (middle set of traces in Figure 5C). Despite the similar amplitude of $[Ca^{2+}]_c$ increase, thapsigargin was much less effective than vasopressin in increasing NAD(P)H levels. In contrast with the observations with hormones, thapsigargin had no effect on NAD(P)H until after a lag of >30 s. Moreover, at the lower level of thapsigargin, the peak amplitude of the redox response was at most 50% of that observed with vasopressin, and in many cells there was no detectable NAD(P)H change, even though $[Ca^{2+}]_c$ increased to a similar level (see mean responses depicted in middle set of traces in Figure 5C). Partial elevation of $[Ca^{2+}]_c$ with low doses of ionomycin was also without effect on mitochondrial redox state (data not shown). These findings emphasize the importance of the IP_3-stimulated Ca^{2+} release pathway in activating mitochondrial metabolism and demonstrate that the mitochondria effectively discriminate fast hormone-induced $[Ca^{2+}]_c$ responses from slow or small amplitude changes in $[Ca^{2+}]_c$.

To investigate further the transmission of $[Ca^{2+}]_c$ signals into the mitochondrial matrix, we established conditions for direct measurements of $[Ca^{2+}]_m$ changes in single hepatocytes loaded with Rhod 2–acetoxymethyl ester (AM) reduced by sodium borohydride (dihydro–Rhod 2–AM) (see Experimental Procedures). Figure 6A shows typical single cell $[Ca^{2+}]_m$ and $[Ca^{2+}]_c$ responses to maximal thapsigargin, with mean responses shown in the inset. These data confirm that the long lag between the $[Ca^{2+}]_c$ and NAD(P)H increases induced by thapsigargin was due to a delayed uptake of Ca^{2+} into the mitochondrial matrix. Evidence that the Rhod 2 signal is derived from the mitochondria comes from the rapid decrease in $[Ca^{2+}]_m$ following uncoupler addition to remove the driving force for $[Ca^{2+}]_m$ accumulation (Figure 6A). By contrast, $[Ca^{2+}]_c$ remained elevated and actually increased transiently during this treatment. The lag between the $[Ca^{2+}]_c$ and $[Ca^{2+}]_m$ increases in the presence of thapsigargin may reflect the slow activation of the Ca^{2+} uniport by $[Ca^{2+}]_c$ (Kröner, 1986; Gunter and Pfeiffer, 1990). This activation is manifest in the micromolar range of Ca^{2+} concentrations and occurs with remarkably slow

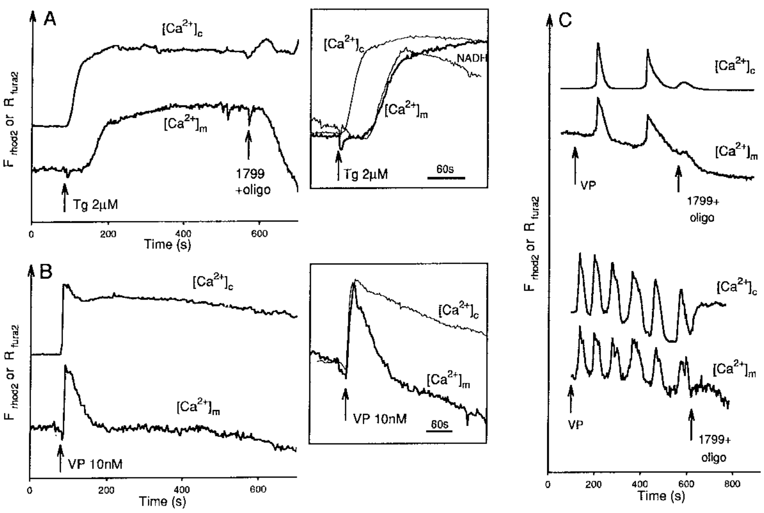

Figure 6. Transmission of $[Ca^{2+}]_c$ Changes into the Mitochondrial Matrix

$[Ca^{2+}]_m$ was monitored in hepatocytes loaded with dihydro-Rhod 2-AM (F_{rhod2}), and $[Ca^{2+}]_c$ was measured in cells loaded with Fura 2-AM (R_{fura2}).

(A) Time courses of $[Ca^{2+}]_c$, $[Ca^{2+}]_m$, and NAD(P)H increases evoked by 2 μM thapsigargin (Tg) were measured under identical conditions in individual hepatocytes from the same culture. The uncoupler 1799 (5 μg/ml) and oligomycin (oligo) (5 μg/ml) were added to demonstrate the mitochondrial localization of the Rhod 2. The inset shows the mean cell population responses to thapsigargin for $[Ca^{2+}]_c$, $[Ca^{2+}]_m$, and NAD(P)H.

(B) $[Ca^{2+}]_c$ and $[Ca^{2+}]_m$ measured separately in single hepatocytes challenged with a maximal (10 nM) dose of vasopressin (VP). The inset shows cell population mean responses for $[Ca^{2+}]_c$ and $[Ca^{2+}]_m$.

(C) Simultaneous measurements of oscillations of $[Ca^{2+}]_c$ and $[Ca^{2+}]_m$ in two single hepatocytes stimulated with 2 nM vasopressin (VP).

kinetics in the lower part of this $[Ca^{2+}]$ range (30–60 s at 2 μM free Ca^{2+}) (Kröner, 1986). Studies using rapid permeabilization of hepatocytes in suspension to measure intracellular Ca^{2+} pool sizes have also demonstrated that thapsigargin causes a relatively slow but prolonged accumulation of Ca^{2+} into the mitochondrial compartment (Hoek et al., 1995). Despite the disparity in the time course of $[Ca^{2+}]_c$ and $[Ca^{2+}]_m$ increase following thapsigargin treatment of hepatocytes, the NAD(P)H increase tracked the rising phase of $[Ca^{2+}]_m$ closely (inset of Figure 6A). This indicates that the CSMDHs were activated in proportion to the accumulation of Ca^{2+} within the mitochondrial matrix. Therefore, it appears that discrimination of $[Ca^{2+}]_c$ signals occurs at the level of mitochondrial Ca^{2+} uptake rather than at the level of Ca^{2+} control of the CSMDHs.

In contrast with the difference in the kinetics of $[Ca^{2+}]_c$ and $[Ca^{2+}]_m$ increase in response to thapsigargin, the rising phase of Ca^{2+} in the two compartments was indistinguishable during vasopressin activation (Figure 6B). This accounts for the much more rapid reduction of the flavin and pyridine nucleotides associated with CSMDH activation during hormonal stimulation. Furthermore, the data of Figure 6B provide direct evidence that the $[Ca^{2+}]_m$ increase is only transient, even when the vasopressin-induced $[Ca^{2+}]_c$ increase is sustained. Finally, the ability to monitor $[Ca^{2+}]_c$ and $[Ca^{2+}]_m$ simultaneously from single cells has allowed us to demonstrate that hormone-induced oscillations of $[Ca^{2+}]_c$ are rapidly transmitted into the mitochondrial matrix (Figure 6C). Thus, each $[Ca^{2+}]_c$ oscillation is accompanied by a parallel spike of $[Ca^{2+}]_m$. These data provide direct evidence that $[Ca^{2+}]_c$ spikes generated by IP_3-dependent release of Ca^{2+} from intracellular stores are efficiently utilized to activate mitochondrial metabolism. This is in marked contrast with the situation with other effectors of $[Ca^{2+}]_c$, which appear to result in inefficient transmission into the mitochondria of hepatocytes.

Mechanism of Oscillatory $[Ca^{2+}]_c$ Signaling to the Mitochondria

A high density of IP_3 receptors has been reported to exist in endoplasmic reticulum domains facing the mitochondria (Satoh et al., 1990; Takei et al., 1992). This may explain the functional observation that agonist-stimulated Ca^{2+} release from intracellular stores is transmitted into the mitochondria much more efficiently than apparently equivalent $[Ca^{2+}]_c$ increases derived by other mechanisms (Rizzuto et al., 1993, 1994; the present study). IP_3-dependent Ca^{2+} mobilization is the primary mechanism by which $[Ca^{2+}]_c$ signals are generated in hepatocytes and in numerous other nonexcitable cells stimulated with inositol lipid-linked agonists. The positive feedback effect of $[Ca^{2+}]_c$ on IP_3-induced Ca^{2+} release gives rise to the rapid-rising phase of both oscillatory and sustained $[Ca^{2+}]_c$ responses

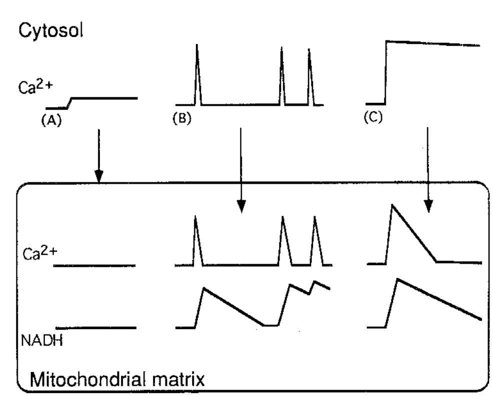

Figure 7. Decoding of $[Ca^{2+}]_c$ Signals by Mitochondria in Hepatocytes

The effects on $[Ca^{2+}]_m$ and the generation of NAD(P)H by CSMDHs are shown for $[Ca^{2+}]_c$ increases that are partial (A), oscillatory (B), and sustained at the peak level (C).

and probably also underlies the regenerative propagation of intracellular Ca^{2+} waves (Rooney and Thomas, 1993). Thus, the kinetics of Ca^{2+} mobilization, together with the colocalization of the Ca^{2+} release sites with the mitochondrial Ca^{2+} uptake sites, may result in locally high elevations of $[Ca^{2+}]_c$ sufficient to facilitate rapid activation of Ca^{2+} uptake into the mitochondria (Rizzuto et al., 1993, 1994). Such local $[Ca^{2+}]_c$ gradients in the immediate vicinity of the mitochondria are not expected when Ca^{2+} stores are mobilized with thapsigargin or ionophore or when the primary source of $[Ca^{2+}]_c$ increase is plasma membrane Ca^{2+} influx. However, it should be noted that voltage-operated Ca^{2+} channels may also be located in a favorable position to control mitochondrial metabolism in some cell types (Pralong et al., 1992, 1994).

The schematic in Figure 7 shows the relationship among $[Ca^{2+}]_c$, $[Ca^{2+}]_m$, and the mitochondrial redox state determined in the present study. Slow or partial elevations of $[Ca^{2+}]_c$ are not readily transmitted into the mitochondrial matrix and are therefore ineffective activators of intramitochondrial metabolism (Figure 7A). In this way the mitochondria can discriminate $[Ca^{2+}]_c$ increases resulting from Ca^{2+} leaks or other effectors of Ca^{2+} homeostasis from IP_3-dependent Ca^{2+} signaling. During the rapid Ca^{2+} mobilization phase of IP_3-mediated $[Ca^{2+}]_c$ oscillations, the proximity of the sites of endoplasmic reticulum Ca^{2+} release and mitochondrial Ca^{2+} uptake results in efficient transmission of the $[Ca^{2+}]_c$ increase into an increase of $[Ca^{2+}]_m$ with similar temporal and spatial organization (Figure 7B). Each spike of $[Ca^{2+}]_m$ increase gives rise to a near-maximal activation of the CSMDHs. The oscillations of $[Ca^{2+}]_m$ follow the same pattern of frequency modulation by agonist dose as the $[Ca^{2+}]_c$ oscillations. Because the mitochondrial redox responses decline relatively slowly, these occur as discrete oscillations only in the lower frequency range and begin to run together when the frequency of $[Ca^{2+}]_m$ spikes is increased. In this way the frequency-modulated $[Ca^{2+}]_m$ signals are translated into a time-averaged redox response, the mean amplitude of which increases with agonist dose. An essentially sustained activation of CSMDHs is achieved within the oscillatory range of $[Ca^{2+}]_c$ and $[Ca^{2+}]_m$ (Figure 7B).

In contrast with the sustained increases of NAD(P)H and $FADH_2$ observed with the upper frequency range of $[Ca^{2+}]_c$ oscillations, sustained $[Ca^{2+}]_c$ increases were associated with only a transient redox response. A similar transient reduction of NAD(P) in response to high levels of Ca^{2+}-mobilizing hormones has been reported in suspensions of hepatocytes (Halestrap, 1989). In the latter study, the declining phase of NAD(P)H was suggested to result from a secondary stimulation of the respiratory chain, resulting from Ca^{2+}-induced inhibition of mitochondrial matrix pyrophosphatase. According to this explanation, the CSMDHs remain activated, but NAD(P)H levels fall owing to enhanced utilization (Halestrap, 1989). However, the present study shows that $[Ca^{2+}]_m$ does not remain elevated during the sustained $[Ca^{2+}]_c$ increase induced by maximal hormone doses. As a result, there is no sustained $[Ca^{2+}]_m$ signal to maintain the activation of CSMDHs under these conditions (Figure 7C). The divergence of the $[Ca^{2+}]_c$ and $[Ca^{2+}]_m$ signals at high hormone doses may result from the dissipation of the locally high levels of $[Ca^{2+}]_c$ once the initial Ca^{2+} mobilization phase is complete. Although $[Ca^{2+}]_c$ levels remain elevated, the rate of Ca^{2+} release from intracellular stores is expected to be much reduced during the plateau phase. Moreover, the IP_3 receptor Ca^{2+} channels become inactivated through an IP_3-dependent and Ca^{2+}-facilitated mechanism that reduces the net permeability by at least 10-fold (Hajnóczky and Thomas, 1994). Thus, the efficient transmission of Ca^{2+} signals into the mitochondria appears to depend on the active mobilization of Ca^{2+} from the intracellular stores, which occurs at a sufficient rate only during the rising phase of $[Ca^{2+}]_c$.

In a recent study, Loew et al. (1994) reported that elevations of $[Ca^{2+}]_c$ in neuroblastoma cells are correlated with a 10–15 mV decrease in mitochondrial membrane potential, which may result from the electrogenic uptake of Ca^{2+}. In contrast with this potential inhibitory effect on ATP generation, the Ca^{2+}-mediated activation of mitochondrial dehydrogenases in hepatocytes results in an increase in NADH supply, which will enhance ATP production and facilitate the transfer of reducing equivalents to the cytosol for utilization in biosynthetic pathways. At the single cell level, CSMDHs appear to be activated to a similar extent by each cycle of Ca^{2+} mobilization, independent of the frequency of the coupled $[Ca^{2+}]_c$ and $[Ca^{2+}]_m$ oscillations. However, the dose-dependent regulation of $[Ca^{2+}]_c$ oscillation frequency by hormones will determine the time-averaged activity of the CSMDHs. Furthermore, the relatively slow decay of the mitochondrial redox potential following each $[Ca^{2+}]_m$ transient will set the frequency range over which this regulation occurs. In asynchronous multicellular systems, the summation of the frequency-modulated responses is expected to yield an apparent steady-state activation of mitochondrial metabolism, the extent of which will be determined by agonist dose. However, in tissues such as the liver, in which hepatocyte $[Ca^{2+}]_c$ oscillations are coordinated through intercellular communication (Robb-Gaspers and Thomas, 1995), the pulsatile nature of the Ca^{2+} signals may be reflected in the metabolic output at subsaturating frequencies of $[Ca^{2+}]_c$ oscillation.

Conclusions

The data presented here establish the concept that the pulsatile organization and frequency modulation of $[Ca^{2+}]_c$ signaling are superior to amplitude modulation of $[Ca^{2+}]_c$ responses in controlling mitochondrial metabolism. This is because the discrete $[Ca^{2+}]_c$ spikes that comprise the $[Ca^{2+}]_c$ oscillations are each delivered efficiently into the mitochondrial matrix. Moreover, the activity of CSMDHs can be regulated over a broad range by the frequency of the oscillating $[Ca^{2+}]_m$ signal. By contrast, the maintained high $[Ca^{2+}]_c$ signals that result from maximal hormonal stimulation can only evoke a transient elevation of $[Ca^{2+}]_m$ and consequently do not sustain the activation of the CSMDHs. Furthermore, slow or partial $[Ca^{2+}]_c$ changes that do not meet the spatial and kinetic requirements for transmission to the mitochondria are filtered out. Therefore, it appears that Ca^{2+} signaling to the mitochondria is tuned to the oscillatory range of $[Ca^{2+}]_c$ signals and that these organelles actually tune out other forms of $[Ca^{2+}]_c$ increase.

Experimental Procedures

Cells

Hepatocytes isolated by collagenase perfusion of the liver from fed male Sprague–Dawley rats were maintained in primary culture for 3–18 hr in Williams' E medium, as described previously (Rooney et al., 1989), except that dexamethasone and insulin were omitted. Prior to use, the cells were washed and preincubated for 40 min in buffer composed of 121 mM NaCl, 5 mM $NaHCO_3$, 10 mM Na–HEPES, 4.7 mM KCl, 1.2 mM KH_2PO_4, 1.2 mM $MgSO_4$, 10 mM glucose, 0.25% BSA (fraction V, Boehringer Mannheim) at pH 7.4. For imaging experiments, 30–100 cells in the microscope field were monitored independently, and all experiments were repeated using at least four separate hepatocyte preparations.

Imaging Measurements of $[Ca^{2+}]_c$ and the Redox State of Pyridine and Flavin Nucleotides

$[Ca^{2+}]_c$ was measured essentially as described previously (Rooney et al., 1989, 1990). In brief, primary culture hepatocytes were loaded with 5 μM Fura 2–AM for 20–30 min in the presence of 100 μM sulfinpyrazone at 37°C. Coverslips with the cultured cells were then inserted into a thermostatically regulated microscope chamber (37°C). Fluorescence images were acquired using a cooled CCD camera under computer control. The computer also controlled a filter wheel to select the excitation wavelength and a stepper motor to select the appropriate dichroic reflector and emission filter. Excitation at 340 and 380 nm was used with a broad band emission filter passing 460–600 nm for measurements of $[Ca^{2+}]_c$ alone. When $[Ca^{2+}]_c$ was measured simultaneously with NAD(P)H and FAD, cells were loaded with Fura 2–AM (1–2 μM) for only 2 min. This loading procedure resulted in a much smaller cellular Fura 2 fluorescence signal than that described above, yielding about the same fluorescence signal as that due to the endogenous NAD(P)H measured at 360 nm excitation. Sulfinpyrazone (100 μM) and TPEN (30 μM) were also present to minimize dye loss and prevent quenching of Fura 2 by heavy metal ions. Excitation at 380 nm, 340 nm, or both were used for Fura 2, and 360 nm excitation was used for NAD(P)H. A broad band emission filter passing 460–600 nm was used with each of these excitation wavelengths. Fura 2 fluorescence is insensitive to Ca^{2+} at 360 nm excitation, so the NAD(P)H signal was generally not contaminated by Ca^{2+} changes. In some cells there was a slight spill over of the signal from the Ca^{2+}-free form of Fura 2, giving a fluorescence decrease during $[Ca^{2+}]_i$ increases (e.g., Figure 1A). FAD fluorescence was measured using 470 nm excitation and 535 nm emission. Acetoacetate (2 mM) was added in some experiments to shift the redox of the mitochondrial flavin and pyridine nucleotides toward a more oxidized state. We also examined the effects of lactate (3 mM) plus pyruvate (0.3 mM) on the hormone-induced redox oscillations. There was no qualitative difference in the pattern of redox responses or $[Ca^{2+}]_c$ oscillations under these different substrate conditions. When NAD(P)H and FAD were measured separately from $[Ca^{2+}]_c$, Fura 2 loading, sulfinpyrazone, and TPEN were omitted. During the initial phase of the redox measurements, there was a relatively rapid partial bleach of autofluorescence. This did not result in a decreased amplitude of the NAD(P)H or FAD signals, but most experiments were preceded by collection of 100 extra images to obtain a stable baseline.

Imaging Measurements of $[Ca^{2+}]_m$

When fluorescent Ca^{2+} indicators are introduced into cells in the AM form, the dye becomes trapped in the cytosol or in intracellular compartments, depending on the place of hydrolysis. Rhod 2–AM has a net positive charge, which facilitates its sequestration into mitochondria due to potential-driven uptake. The use of dihydro–Rhod 2–AM enhances the selectivity for mitochondrial loading because this dye exhibits Ca^{2+}-dependent fluorescence only after it is oxidized and this occurs preferentially within the mitochondria. Hepatocytes were loaded with 1–2 μM dihydro–Rhod 2–AM in the presence of 2 mM acetoacetate for 60 min. The residual cytosolic fraction of the dye was essentially eliminated when the cells were kept in primary culture for an additional 12–16 hr after loading, whereas the mitochondrial dye fluorescence was maintained. Fluorescence images of Rhod 2 were acquired using 535 nm excitation and 590 nm emission. The mitochondrial localization of the dye was checked by abolishing the driving force for mitochondrial Ca^{2+} uptake using a combination of the uncoupler 1799 and the ATPase inhibitor oligomycin (5 μg/ml each). $[Ca^{2+}]_c$ was transiently increased or unaffected by these agents. Therefore, the inhibition of the Ca^{2+} increases detected by Rhod 2 in the presence of 1799 plus oligomycin indicates the mitochondrial localization of the dye signals. The fluorescence of Rhod 2 was was not calibrated in terms of $[Ca^{2+}]_m$, since it is not a ratiometric dye and is localized in only a small compartment within the cell.

Acknowledgments

Correspondence should be addressed to A. P. T. The authors would like to thank Drs. Jan Hoek, Suresh Joseph, Dick Denton, Andrew Halestrap, and Guy Rutter for helpful discussions. This work was supported by National Institutes of Health grants DK38422 and AA07215 and by Research Scientist Development Award grant AA00180 to A. P. T.

Received April 17, 1995; revised June 19, 1995.

References

Anwer, M. S. (1994). Mechanism of activation of the Na^+/H^+ exchanger by arginine vasopressin in hepatocytes. Hepatology *20*, 1309–1317.

Bachs, O., Agell, N., and Carafoli, E. (1992). Calcium and calmodulin function in the cell nucleus. Biochim. Biophys. Acta *1113*, 259–270.

Denton, R. M., and McCormack, J. G. (1980). On the role of calcium transport in heart and other mammalian mitochondria. FEBS Lett. *119*, 1–8.

Gunter, T. E., and Pfeiffer, D. R. (1990). Mechanisms by which mitochondria transport calcium. Am. J. Physiol. *258*, C755–C786.

Hajnóczky, G., and Thomas, A. P. (1994). The inositol trisphosphate receptor calcium channel is inactivated by inositol trisphosphate. Nature *370*, 474–477.

Halestrap, A. P. (1989). The regulation of the matrix volume of mammalian mitochondria *in vivo* and *in vitro* and its role in the control of mitochondrial metabolism. Biochim. Biophys. Acta *973*, 355–382.

Hansford, R. G. (1980). Control of mitochondrial substrate oxidation. Curr. Topics Bioenerg. *10*, 217–277.

Hoek, J. B., Farber, J. L., Thomas, A. P., and Wang, X. (1995). Calcium ion–dependent signalling and mitochondrial dysfunction: mitochondrial calcium uptake during hormonal stimulation in intact liver cells and its implication for the mitochondrial permeability transition. Biochim. Biophys. Acta, in press.

Kröner, H. (1986). Ca^{2+} ions, an allosteric activator of calcium uptake in rat liver mitochondria. Arch. Biochem. Biophys. *251*, 525–535.

Lin, C., Hajnóczky, G., and Thomas, A. P. (1994). Propagation of cytosolic calcium waves into the nuclei of hepatocytes. Cell Calcium *16*, 247–258.

Loew, L. M., Carrington, W., Tuft, R. A., and Fay, F. S. (1994). Physiological cytosolic Ca^{2+} transients evoke concurrent mitochondrial depolarizations. Proc. Natl. Acad. Sci. USA *91*, 12579–12583.

McCormack, J. G., Halestrap, A. P., and Denton, R. M. (1990). Role of calcium ions in regulation of mammalian intramitochondrial metabolism. Physiol. Rev. *70*, 391–425.

Meyer. T., and Stryer. L. (1991). Calcium spiking. Annu. Rev. Biophys. Biophys. Chem. *20*, 153–174.

Mix, T. C. H., Drummond, R. M., Tuft, R. A., and Fay, F. S. (1994). Mitochondria in smooth muscle sequester Ca^{2+} following stimulation of cell contraction. Biophys. J. *66*, A97.

Miyata, H., Silverman, H. S., Sollott, S. J., Lakatta, E. G., Stern, M. D., and Hansford, R. G. (1991). Measurement of mitochondrial free Ca^{2+} concentration in living single cardiac myocytes. Am. J. Physiol. *261*, H1123–H1134.

Nichols, B. J., Rigoulet, M., and Denton, R. M. (1994). Comparison of the effects of Ca^{2+}, adenine nucleotides and pH on the kinetic properties of mitochondrial NAD^+-isocitrate dehydrogenase and oxoglutarate dehydrogenase from the yeast *Saccharomyces cerevisiae* and rat heart. Biochem. J. *303*, 461–465.

Pralong, W. F., Hunyady, L., Várnai, P., Wollheim, C. B., and Spät, A. (1992). Pyridine nucleotide redox state parallels production of aldosterone in potassium-stimulated adrenal glomerulosa cells. Proc. Natl. Acad. Sci. USA *89*, 132–136.

Pralong, W. F., Spät, A., and Wollheim, C. B. (1994). Dynamic pacing of cell metabolism by intracellular Ca^{2+} transients. J. Biol. Chem. *269*, 27310–27314.

Rapp, P. E., and Berridge, M. J. (1981). The control of transepithelial potential oscillations in the salivary gland of *Calliphora erythocephala.* J. Exp. Biol. *93*, 119–132.

Rizzuto, R., Simpson, A. W. M., Brini, M., and Pozzan, T. (1992). Rapid changes of mitochondrial Ca^{2+} revealed by specifically targeted recombinant aequorin. Nature *358*, 325–327.

Rizzuto, R., Brini, M., Murgia, M., and Pozzan, T. (1993). Microdomains with high Ca^{2+} close to IP_3-sensitive channels that are sensed by neighboring mitochondria. Science *262*, 744–746.

Rizzuto, R., Bastianutto, C., Brini, M., Murgia, M., and Pozzan, T. (1994). Mitochondrial Ca^{2+} homeostasis in intact cells. J. Cell Biol. *126*, 1183–1194.

Robb-Gaspers, L. D., and Thomas, A. P. (1995). Coordination of Ca^{2+} signaling by intercellular propagation of Ca^{2+} waves in the intact liver. J. Biol. Chem. *270*, 8102–8107.

Robitaille, R., Adler, E. M., and Charlton, M. P. (1990). Strategic localization of calcium channels at transmitter release sites of frog neuromuscular synapses. Neuron *5*, 773–779.

Rooney, T. A., and Thomas, A. P. (1993). Intracellular calcium waves generated by Ins(1,4,5)P_3-dependent mechanisms. Cell Calcium *14*, 673–690.

Rooney, T. A., Sass, E., and Thomas, A. P. (1989). Characterization of cytosolic calcium oscillations induced by phenylephrine and vasopressin in single fura-2-loaded hepatocytes. J. Biol. Chem. *264*, 17131–17141.

Rooney, T. A., Sass, E., and Thomas, A. P. (1990). Agonist-induced cytosolic calcium oscillations originate from a specific locus in single hepatocytes. J. Biol. Chem. *265*, 10792–10796.

Satoh, T., Ross, C. A., Villa, A., Supattapone, S., Pozzan, T., Snyder, S. H., and Meldolesi, J. (1990). The inositol 1,4,5-trisphosphate receptor in cerebellar Purkinje cells: quantitative immunogold labeling reveals concentration in an ER subcompartment. J. Cell Biol. *111*, 615–624.

Scholz, R., Thurman, R. G., Williamson, J. R., Chance, B., and Bücher, T. (1969). Flavin and pyridine nucleotide oxidation-reduction changes in perfused rat liver. J. Biol. Chem. *244*, 2317–2324.

Takei, K., Stukenbrok, H., Metcalf, A., Mignery, G. A., Südhof, T. C., Volpe, P., and De Camilli, P. (1992). Ca^{2+} stores in Purkinje neurons: endoplasmic reticulum subcompartments demonstrated by the heterogeneous distribution of the $InsP_3$ receptor, Ca^{2+}-ATPase, and calsequestrin. J. Neurosci. *12*, 489–505.

Thomas, A. P., Renard, D. C., and Rooney, T. A. (1992). Spatial organization of Ca^{2+} signalling and Ins(1,4,5)P_3 action. Adv. Second Messenger Phosphoprotein Res. *26*, 225–263.

Woods, N. M., Cuthbertson, K. S. R., and Cobbold, P. H. (1986). Repetitive transient rises in cytoplasmic free calcium in hormone-stimulated hepatocytes. Nature *319*, 600–602.